Interference of Acoustic Signals Due to Internal Waves in Shallow Water

Young-Nam Na

(Agency for Defense Development, Chinhae 645-600, Korea)

ABSTARCT

To investigate internal waves (IW) effect on acoustic wave propagation, an analysis is conducted on mode travel time and model simulation. Based on the thermistor string data, it can be shown that the thermocline depth variation may cause travel time difference as much as 4-10 ms between mode 1 and 2 over range 10 km. This travel time difference causes interference among modes and thus fluctuation from range-independent stratified ocean structure. In real situations, however, there exist additionally spatial variation of IW. Model simulation with all modes and simple IW shows clear responses of acoustic signals to IW, amplitude and phase fluctuation.

INTRODUCTION

Whenever a sufficient vertical density gradient exists in ocean, internal waves (IW) restored by buoyancy can occur. Because they owe their existence to the restoring force due to the density gradient and the Coriolis force, the frequency spectra of IW are bounded by the inertial frequency at the low end and by the buoyancy frequency at the high end. IW are characterized by temperature and velocity fluctuations with periods of tens of seconds to several hours, and with scales from 100 m to 10 km in the horizontal, 1 to 100 m in the vertical. They are important mechanisms for mixing and energy transport in both the shallow and the deep ocean [1].

Acoustically, temperature fluctuation causes changes in sound speed, which in turn lead to the fluctuations of travel time of pulse signal. Internal wave-induced ocean variability in temporal and spatial domain has been found to be a very significant source of sound scattering and has received considerable attention in recent years..

This paper delivers travel time difference based on the thermistor string data and experimental conditions. And the fluctuation of acoustic pressure fields due to simple IW is simulated using the model, RAM [2], which is based on the parabolic equation technique.

SEA EXPERIMENT

In order to investigate the characteristics of IW, sea experiments were conducted in the East Sea off Donghae city in October 1997 and June 1998. Figure 1 shows the locations where equipment were installed during the experiments. In 1998, two thermistor strings, each having 9 temperature

sensors every 10 m, were deployed to estimate the direction and the speed of IW. The water depth varies from 130 m to 140 m. The thermistor strings (TR7-1,2) were designed to gather data every 10 sec. The oceanographic experiments were performed at the same location TR7-2 in 1977 and at the locations TR7-1, 2 in 1998. There was actually no wind (wave-height was below 0.5 m) so that the weather allowed very nice condition to perform the experiments.

MODE ARRIVING STRUCTURE

To estimate travel time difference of acoustic waves due to IW variation, this study employs the simplified formula based on the ray-mode theory. The normal mode theory is widely accepted in calculating the sound pressure fields. The mode eigenfunction and wavenumber are two important components analyzing propagating fluctuation. The ray-mode theory can give very intuitive idea of acoustic responses to thermocline. Zhang et al. [3] presented the simplified formula of the horizontal wavenumbers and the group velocities from the ray-mode theory. Here, we briefly describe the formula.

The grazing angle of θ_l of the eigenray of the l-th mode satisfies the following equation.

$$k_0 \cos\theta_l = \mu_l , \qquad (1)$$

where $k_o = \omega / c_o$, and μ_l is the eigenvalue which can be estimated from the equation of eigenvalue as shown

$$2\sqrt{k_0^2 - \mu_l^2}\,h = 2(l-1)\pi + \frac{\pi}{2} + \varphi_b(\mu_l), \quad (2)$$

where h is the thickness of water below the thermocline as shown in Fig. 2, and φ_b is the phase shift at the bottom. Thus the group velocity can be expressed as following :

$$v_l = c_0 \cos\theta_l = c_0\sqrt{1-\left[\frac{2(l-1)\pi + \pi/2 + \varphi_b(\mu_l)}{4}\frac{c_0}{fh}\right]^2} \quad .(3)$$

It is clear that the thermocline depth is critical to group velocities. For the several modes, where the grazing angles of the corresponding energy are small, the asymptotical formula for group velocities can be used and $\varphi_b(\mu_l)$ can be fixed to $\pi/2$ for simplicity. The time delay between mode 1 and mode l at range r is then expressed as :

$$\tau_{1l} = r\left[v_l^{-1} - v_1^{-1}\right] \approx \frac{1}{32}\frac{rc_0}{f^2h^2}\left[(2l-1)^2 - 1\right]. \quad (4)$$

and the influence of the thermocline depth variation on time delay variation is derived by taking derivative of τ with respect to h, which is

$$\left|\frac{\partial\tau_{1l}}{\partial h}\right| \approx \frac{1}{16}\frac{rc_0}{f^2h^3}\left[(2l-1)^2 - 1\right]. \qquad (5)$$

Here, the thermocline depth h, which is a function of time, is obtained by finding the depth of temperature 6℃ from the thermistor string data. The temperature 6℃ is assumed to be the lower limit of thermocline depth.

It can be seen from Eq. 4 that the group velocities are closely dependent on the thermocline

depth. The group delay varies inverse proportionally to the square of the depth of the thermocline and the square of signal frequency. So, the smaller h is, the greater the group delay variation will be. Assuming the water depth to be 140 m, one may obtain the depth h below the thermocline as 110 m. When the temperature is 6 °C, the simple formula [4] leads to sound velocity of about 1476 m/s at depth 100 m. Assuming r = 10 km and f = 250 Hz, the travel time difference between the first two modes and its depth derivative at 250 Hz are computed as 4.9 ms and 0.1 ms/m, respectively.

Figure 3 shows the travel time difference τ_{12} between mode 1 and 2, which is calculated using Eq. (4). Here, the source-receiver range is assumed to be 10 km and the frequency 250 Hz. The thermocline depth h is obtained via interpolating the isothermal depth of 6 °C from the four temperature data. From the temperature profile at the source, one can see that the depth corresponding to 6 °C is roughly lower limit of thermocline. Since the sampling interval is 10 sec, the time sequence 1800 yields 18000 sec or 5 hours. The first two curves (Fig. 3a) shows that they vary within some range of variation, 9-12 ms. Between the last two curves (Fig. 3b), however, there exist large difference reaching almost 3.0 ms at time sequence 2400. Noticing the fact that the first two data have same position with one day jump but the second two data have same time with 1.3 km away, one can see that travel time difference (or thermocline depth) varies more with space than with time.

Table 1 summarizes statistical characteristics of thermocline depth and travel time difference for the four data sets. The variance of thermocline depth reaches up to 33 m at TR7-1 (June 1, 1998). Meanwhile, that of travel time difference between mode 1 and 2 varies from 0.12 ms to 0.56 ms over range 10 km. This travel time difference causes interference among modes and thus fluctuation from (range-independent) stratified ocean structure. This simple calculation here considers only time variation effect of thermocline (i.e., IW variation at one point). In real situations, however, there exist additional spatial variation of IW. The following section considers the spatial effect of IW on acoustic wave propagation through model simulations.

MODEL SIMULATION

A. Model Input

To simulate the spatial variation of pressure fields due to IW, a set of IW is generated as following formula :

$$z(d) = d - A(d)\sin(2\pi r / \lambda_f). \qquad (6)$$

where $z(d)$ = depth variation, d = depth of IW, r = horizontal range, λ_f = wavelength. The amplitude $A(d)$ is defined as $10\cos(|20-d|\pi/20)$, where d exists between 10 m and 30 m. The IW consist of five waves of each wavelength 200 m so that they covers horizontal range of 1 km, starting at the range 1 km. Figure 4 shows the input sound speed structure with IW characteristics.

As for geoacoustic data, the parameters of sand-silt-clay are considered. The typical values are sound velocity c_b = 1500 m/s, density ρ_b = 1500 kg/m^3, and attenuation α_b = 0.8 dB/λ [5]. The water depth is 140 m and the sound source is

located at 20 m, the center depth of IW.

B. Model

The model RAM (range-dependent acoustic model) is based on the parabolic equation (PE) technique. The PE method is very effective for solving range-dependent ocean problems. RAM was developed using the split step Pade' solution [6], which allows large range steps and is the most effective PE algorithm that has been developed. We just describe final results of pressure fields in range-independent case.

In cylindrical coordinates, the pressure field in range increment Δr can be obtained as following :

$$p(r+\Delta r, z) = \exp(ik_o \Delta r)\left(1 + \sum_{j=1}^{n} \frac{\gamma_{j,n} X}{1+\beta_{j,n} X}\right) p(r, z), \quad (7)$$

where the operator

$$X = k_o^{-2}\left(\rho \frac{\partial}{\partial z}\frac{1}{\rho}\frac{\partial}{\partial z} + k^2 - k_o^2\right),$$
$$k_o = \omega / c_o . \quad (8)$$

and c_o is a representative phase speed. The complex coefficients $\gamma_{j,n}$, $\beta_{j,n}$ are defined by placing accuracy and stability constants on the rational function.

The self starter for a point source is employed in the form

$$p(r_o, z) = \frac{\exp\left(ik_o r_o (1+X)^{1/2}\right)}{k_o^{1/2}(1+X)^{1/4}} \delta(z - z_o). \quad (9)$$

To avoid encountering singular intermediate solutions, RAM solves Eq. (9) with the following approach :

$$(1-X)^2 q(z) = k_o^{-1/2} \delta(z - z_o). \quad (10)$$
$$p(r_o, z) = (1+X)^{7/4} \exp\left(ik_o r_o (1+X)^{1/2}\right) q(z). \quad (11)$$

The intermediate function q has two continuous derivatives. The depth operator X is discretized using Galerkin's method as described in [7]. In RAM version 1.0, the factor $(1+X)^2$ was used to smooth the delta function. In later version, however, it was replaced by the factor $(1-X)^2$. This change directs more improved stability. The factor $(1+X)^2$ is nearly singular for some problems involving deep water and/or weak sediment attenuation coefficients.

For range-dependent problems, it is necessary to specify a condition at the vertical interfaces between regions. That is, accurate solutions may be obtained by conserving energy flux, and thus by modifying operator X.

C. Results

Figure 5 shows two distributions of propagation loss when the IW exist and when there are no IW. The sound source is located at depth 20 m and its frequency is 1 kHz. It can be seen that the two results give exactly same distribution until the range 1 km, where the IW start, but give some difference thereafter. That is, the regions marked as 'A', which represents convergence zones of acoustic energy, appear to be distorted when the

IW exist. At near the bottom, acoustic energy bundles marked as 'B' show significant difference between the two cases. Examining the propagation loss difference at some receiver depths (Fig. 6), one can see IW effects on acoustic wave propagation. At receiver depth 20 m with no IW, very regular surface convergence zones develop every 1.4 km. With the IW, however, these convergence zones tend to be distorted and the degree increases as the range increases. At receiver depth 140 m, the bottom, one can find no prominent convergence zones. Instead, irregular fluctuations exist with range. The amplitudes seem to be out of phase between the two curves, resulting in more than 10 dB difference at some ranges. When the source is located within IW, acoustic waves proved to undergo additional interference, which causes difference in magnitudes and phases of their pressure fields.

When the source depth changes into 80 m, below the thermocline, the distributions of propagation loss (Fig. 7) show significant difference compared with the case of source depth 20 m. The most noticeable point is that the acoustic energy seems to be trapped below the thermocline. As a result, no surface convergence zones are formed. This is comprehensible because most of acoustic waves refract down in the thermocline layer and thus few of them 'feel' the IW during propagation.

The model simulation includes all of the possible modes while the travel time estimation in the previous section is attempted for the first two modes. Moreover, the estimation is made for the case when the source exists on the bottom. If the travel time variance is estimated including all the modes, it may give larger value. (Even larger value is expected when the sound source exists within IW!) The travel time fluctuations of acoustic wave due to IW may cause interference between modes.

CONCLUSIONS

Based on the thermistor string data, mode arriving structures are analyzed. As thermocline depth varies with time at one point, it may cause travel time difference as much as 4-10 ms between mode 1 and 2 over range 10 km. This travel time difference causes interference among mode. At one time, IW have their variation in space that lead to acoustic signal fluctuations. Model simulation with all modes and simple IW shows clear responses of acoustic signals to IW, amplitude and phase fluctuation.

Further studies should be followed to investigate spatial features such as propagating direction and wavelengths. To have more productive results on IW effects on acoustic signal propagation, joint experiments of oceanography and acoustics are highly required.

REFERENCES

[1] C. Garret and W. Munk, "Internal waves in the ocean, "*Ann. Rev. Fluid Mech.* Vol. 11, pp. 339-69, 1979.

[2] M. D. Collins, User's Guide for RAM Version 1.0 and 1.0p, Document of Naval Research Laboratory, pp. 1-13, 1997.

[3] R. H.Zhang, J. Q. Ziao and M. Gong, "Analysis of individual modes in shallow water, "*Chinese Journal of Acoustics*, Vol. 3(3), pp. 238-249, 1984.

[4]. C. C. Leroy, "Development of Simple Equations for Accurate and More Realistic Calculation of the Speedd of Sound in Sea Water, " *J. Acoust. Soc. Am.*, Vol. 46, p. 216, 1969.

[5]. J. F. Miller and S. N. Wolf, Modal Acoustic Transmission Loss (MOATAL) : A Transmission – Loss Computer Program Using a Normal-Mode Model of the Acoustic Field in the Ocean, Naval Research Lab., Rep. No. 8429, pp. 1-126, 1980.

[6]. M. D. Collins, "Generalization of the split-step Pada' solution, " *J. Acoust. Soc. Am.* Vol. 96, pp. 382-385, 1993.

[7] M. D. Collins and E. K. Westwood, "A higher-order energy-conserving parabolic equation for range-dependent ocean depth, sound-speed, and density, "*J. Acoust. Soc. Am.*, Vol. 89, pp. 1068-1075, 1991.

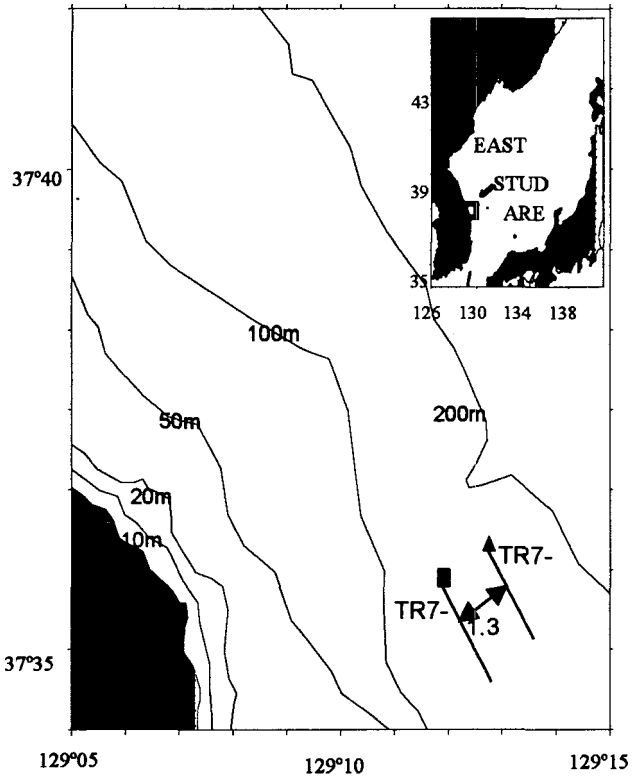

Fig. 1. Station map of oceanographic experiments.

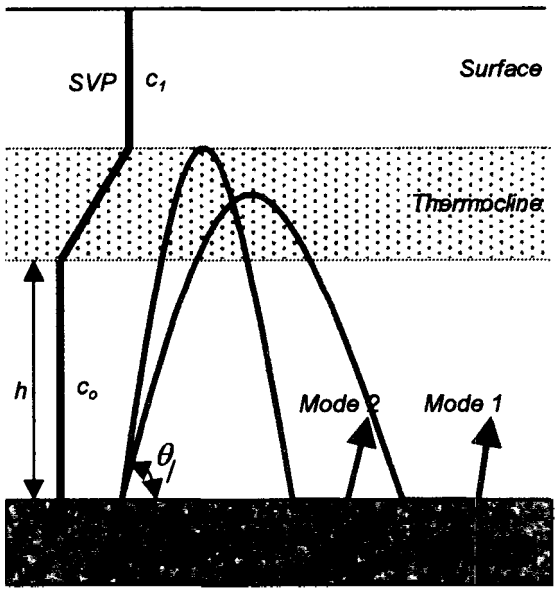

Fig. 2. Schematic picture showing the mode propagation through thermocline.

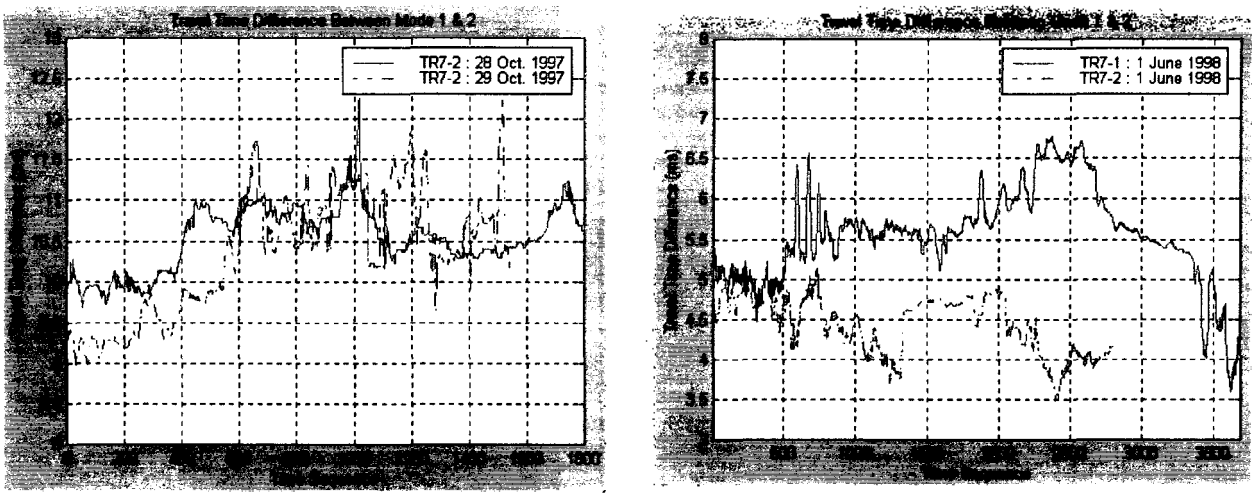

(a) (b)

Fig. 3. Travel time difference (τ_{12}) with time sequence, where the difference is between mode 1 and mode 2. The range r is assumed to be 10 km and the frequency 250 Hz. (a) 28-29 Oct. 1997, (b) 1 June 1998.

Table 1. Mean and variance of thermocline depth (h) and travel time difference (τ_{12}) between mode 1 and 2, where r = 10 km and f = 250 Hz.

	TR7-2 (28 Oct. 1997) Mean	Var.	TR7-2 (29 Oct. 1997) Mean	Var.	TR7-1 (1 June 1998) Mean	Var.	TR7-2 (1 June 1998) Mean	Var.
Thermocline Depth, h	74.88	1.94	75.66	7.67	103.52	33.32	115.70	22.72
Travel Time Difference, τ_{12}	10.54	0.15	10.36	0.56	5.56	0.34	4.43	0.12

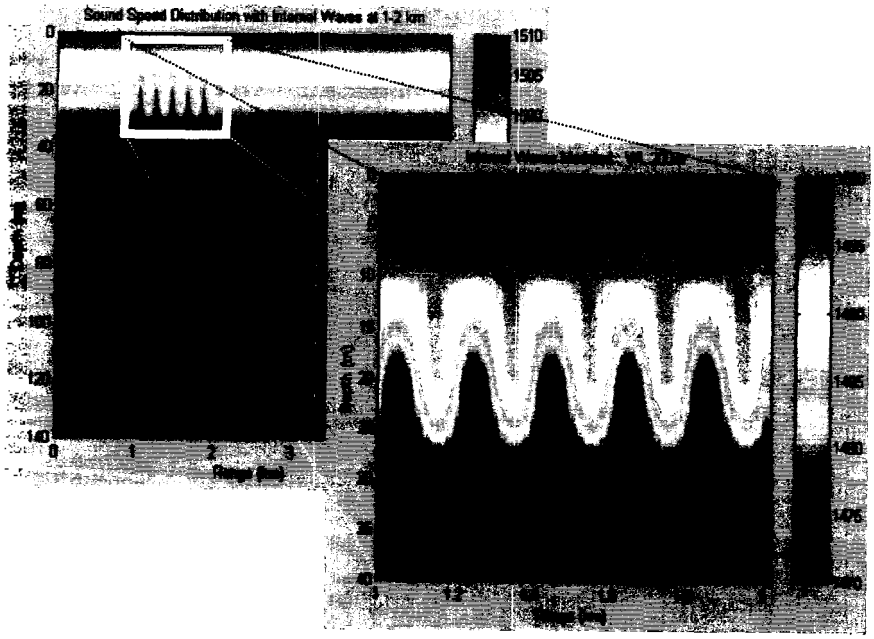

Fig. 4. Internal waves characteristics for the model simulation. The internal waves start at 1km and end at 2km (5 waves), where their wavelength is 200m. The center axis exists on the depth of 20m and the amplitude is 10m.

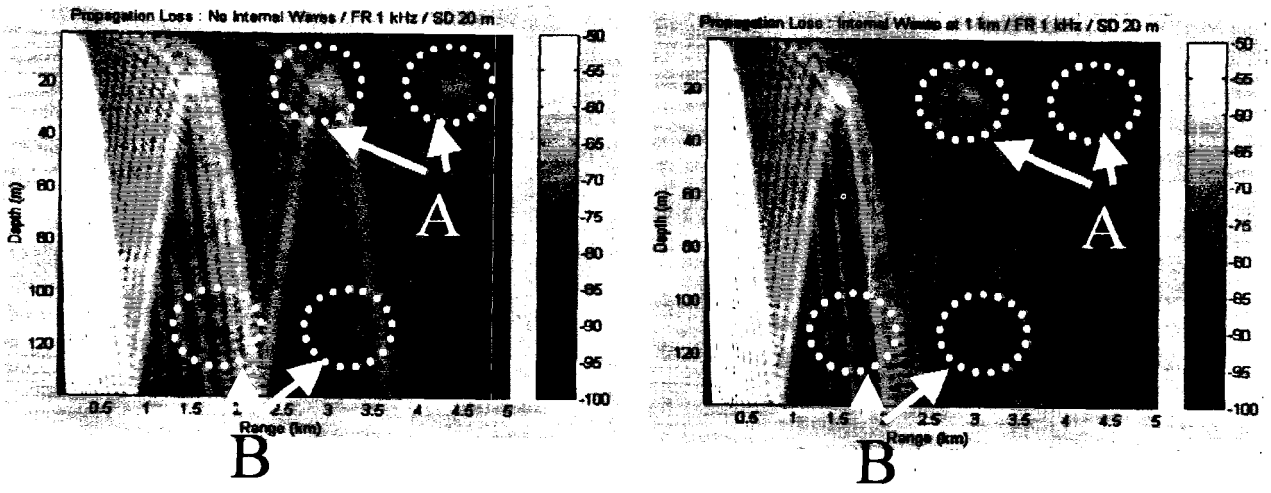

(a) (b)

Fig. 5. Propagation loss variation when the source exists in the IW (SD 20m). (a) no IW, (b) IW.

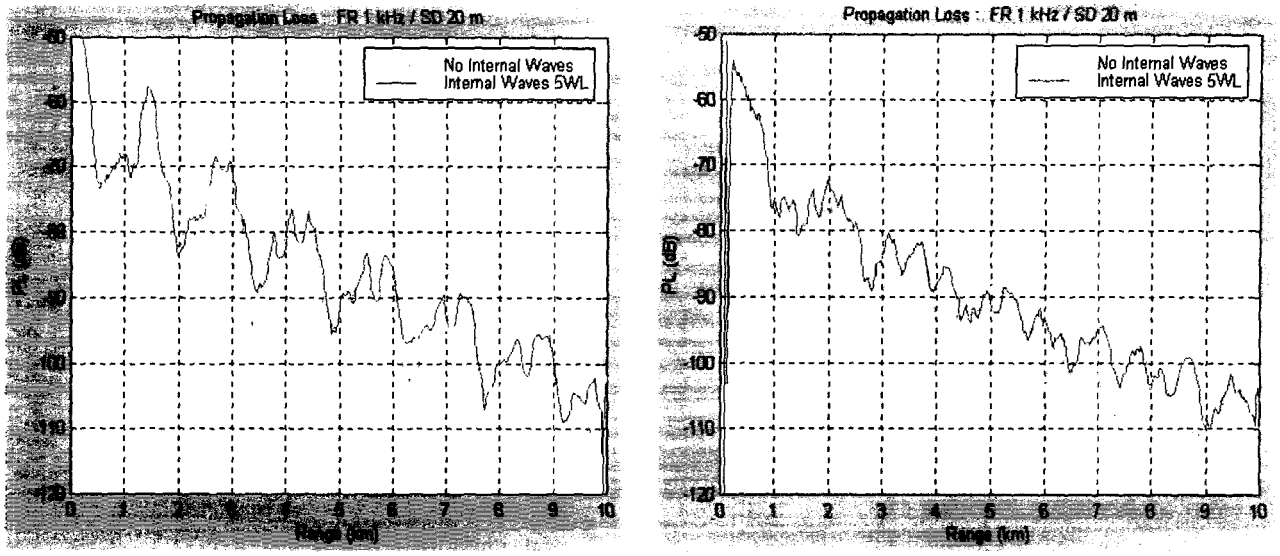

(a) (b)

Fig. 6. Propagation loss at some receiver depths when the source exists in the IW (SD 20 m). (a) 20m, (b) 140m.

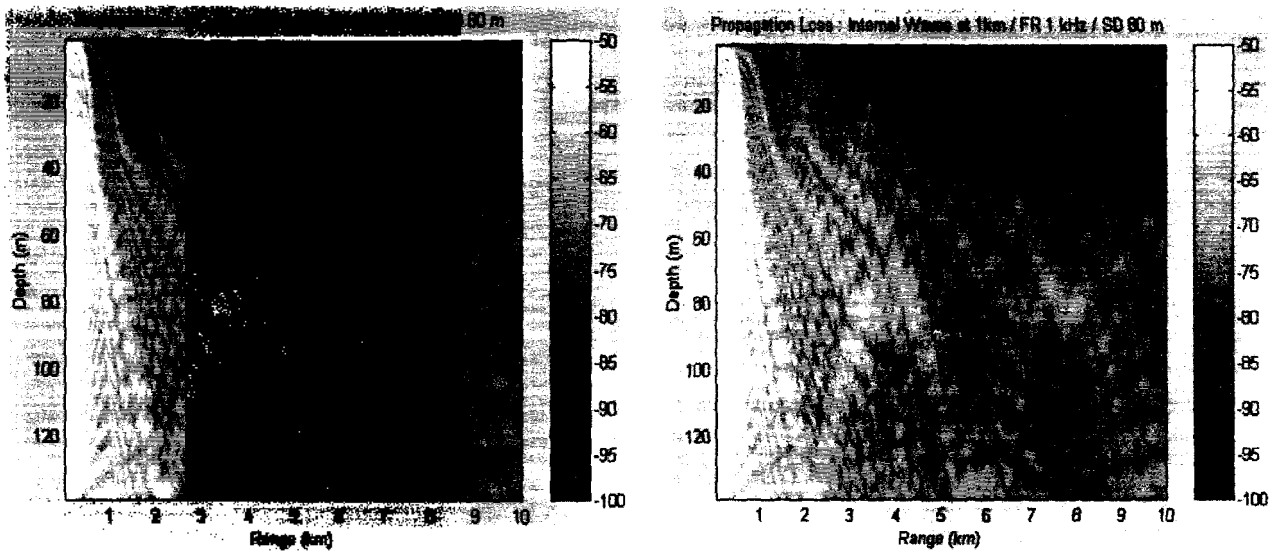

(a) (b)

Fig. 7. Propagation loss variation when the source exists below the IW (SD 80 m). (a) no IW, (b) IW.